Disequilibrium textures in lower crustal rocks of the Sveconorwegian orogen, south-west Sweden

Bettina Richter & Uwe Altenberger

november 2013

SGU-rapport 2013:15

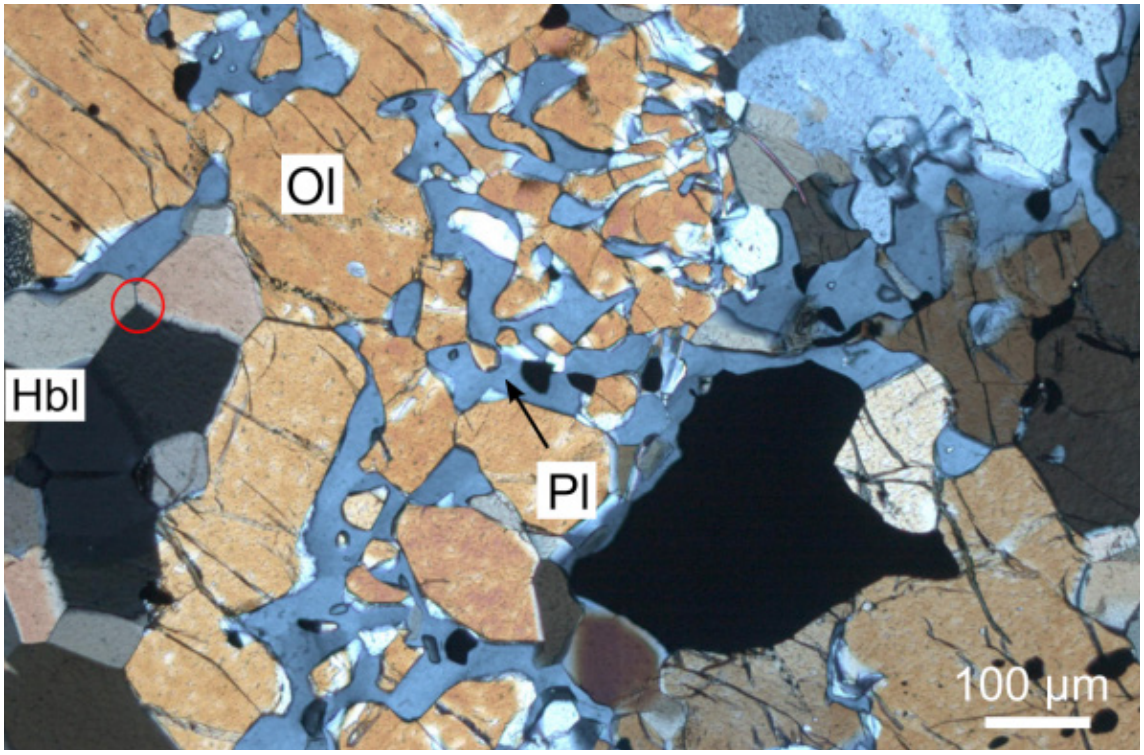

SGU
Sveriges geologiska undersökning
Geological Survey of Sweden

Sveriges geologiska undersökning
Box 670, 751 28 Uppsala
tel: 018-17 90 00
fax: 018-17 92 10
e-post: sgu@sgu.se
www.sgu.se

PREFACE

The work presented in this report was done in conjunction but not cooperation with a regular mapping project by the Geological Survey of Sweden. Its statements and conclusions are solely those of the authors. Limited linguistic and technical editing was performed by Magnus Ripa and Jeanette Bergman Weihed, Geological Survey of Sweden.

CONTENTS

Disequilibrium textures in lower crustal rocks of the Sveconorwegian orogen, south-west Sweden

Bettina Richter* [a,b] & Uwe Altenberger[a]

a Institute of Earth and Environmental Science, Potsdam University, Karl-Liebknecht-Strasse 24, 14476 Potsdam, Germany
b Present address: Department of Environmental Sciences, Basel University, Bernoullistrasse 32, 4056 Basel, Switzerland
* E-mail address: Bettina.Richter@unibas.ch

ABSTRACT

The southern part of the Proterozoic Eastern Segment of the Sveconorwegian orogen in south-west Sweden has had a complex metamorphic and magmatic evolution during which rocks were overprinted by multiple high-temperature and high-pressure events. Locally, however, relict magmatic fabrics and minerals are still preserved. Typical examples of such local disequilibrium textures may be found at lake Skärsjö in garnet-bearing metagabbros which carry magmatic olivine (Fa53Fo47) and plagioclase (An12-19), that was re-equilibrated under metamorphic conditions.

Metamorphic reactions led to the formation of corona textures between the primary magmatic phases. Two kinds of metamorphic coronas developed around the magmatic phases. In the first, magmatic plagioclase was surrounded by small, newly formed garnets. In the second, a small rim of plagioclase formed around olivine and magmatic orthopyroxene. In addition, symplectitic intergrowths of olivine and plagioclase, as well as plagioclase and garnet occur. Biotite and hornblende formed rims around ilmenite and magnetite.

Fortunately, magmatic as well as metamorphic orthopyroxenes coexist permitting the determination of the metamorphic conditions that prevailed during the formation of the corona structures. Some orthopyroxenes are encrusted with garnet, hornblende and metamorphic plagioclase, whereas others overgrew magmatic olivine.

Based on the observed mineral assemblages, textures and calculated P-T conditions (11–14 kbar, 700–750 °C) several stages of the prograde rock evolution have been recognised.

Keywords: Sveconorwegian orogen, Eastern Segment, magmatic fabrics, granulites, disequilibrium textures

INTRODUCTION

The metamorphic rocks of south-west Sweden predominantly have magmatic protoliths that have been reworked since the time of their intrusion (e.g. Andersson et al. 2008). Those of the Eastern Segment of the Sveconorwegian orogen were overprinted by several high-grade metamorphic events, but evidence for magmatic fabrics within garnet-orthopyroxene-bearing amphibolites in the Ullared region in the form of well-preserved coronas between plagioclase and oxides and plagioclase and olivine are locally present. Similar textures have been documented in the Adirondack mountains region, New York (Whitney & McLelland 1972, Whitney & McLelland 1983, Johnson & Carlson 1990), in the Bamble Terrane, Norway (Haas et al. 2002) and in the Jotun Nappe, Norway (Griffin 1971).

The aim of this study is to describe the occurrence of the magmatic relics, the corona-forming metamorphic reactions and the metamorphic conditions during corona growth in the southern part of the Eastern Segment.

REGIONAL GEOLOGY

The Proterozoic rocks of south-west Sweden is part of the Sveconorwegian orogen, which is composed of five principal units. These are from east to west: the Eastern Segment, the Idefjorden Terrane, the Bamble Terrane, the Kongsberg Terrane and the Telemark Terrane (Andersson et al. 2008). The terranes are separated by roughly north–south oriented deformation zones such as the Protogine Zone at the easternmost boundary and the Mylonite Zone between the Eastern Segment and the Idefjorden Terrane (Andersson et al. 2008). The Sveconorwegian orogenesis caused metamorphic overprinting, deformation and magmatic events at different intensities in the terranes between 1.14 and 0.90 Ga (Bingen et al. 2008b).

The study area of the present investigation lies in the Eastern Segment, which is interpreted as the reactivated margin of Fennoscandia (Möller 1998). The Eastern Segment consists of orthogneisses with protolith ages of 1850–1660 Ma (e.g. Söderlund et al. 1999, 2002, Möller et al. 2007, Bingen et al. 2008a). These rocks have compositions similar to those of undeformed intrusive rocks of the Transscandinavian Igneous Belt further east (e.g. Söderlund et al. 1999, Möller et al. 2007). South of lake Vänern, the Eastern Segment consists of orthogneisses including metabasic rocks (Andersson et al. 2008). The orthogneisses were extensively migmatised during an amphibolite-facies metamorphic event, the Hallandian, dated at 1460–1420 Ma (metamorphic zircons, Christoffel et al. 1999, Söderlund et al. 2002, Möller et al. 2007). Sveconorwegian metamorphic conditions range from upper amphibolite to high-pressure granulite facies (680–770 °C and 9–12 kbar, Johansson et al. 1991, Möller 1998). There is evidence for eclogite-facies origin in some mafic high-pressure granulites (Möller 1998). These eclogites were retrogradely overprinted under amphibolite-facies conditions and occur in less deformed rocks in the Ullared Deformation Zone (Fig. 1, Möller 1998).

THE AMPHIBOLITES OF LAKE SKÄRSJÖ

South of the Ullared Deformation Zone, c. six kilometres south of Gällared at lake Skärsjö, a large outcrop of amphibolites is situated along the road at the southern part of the lake (Fig. 2). The amphibolites are part of a mafic lens within various orthogneisses. The western

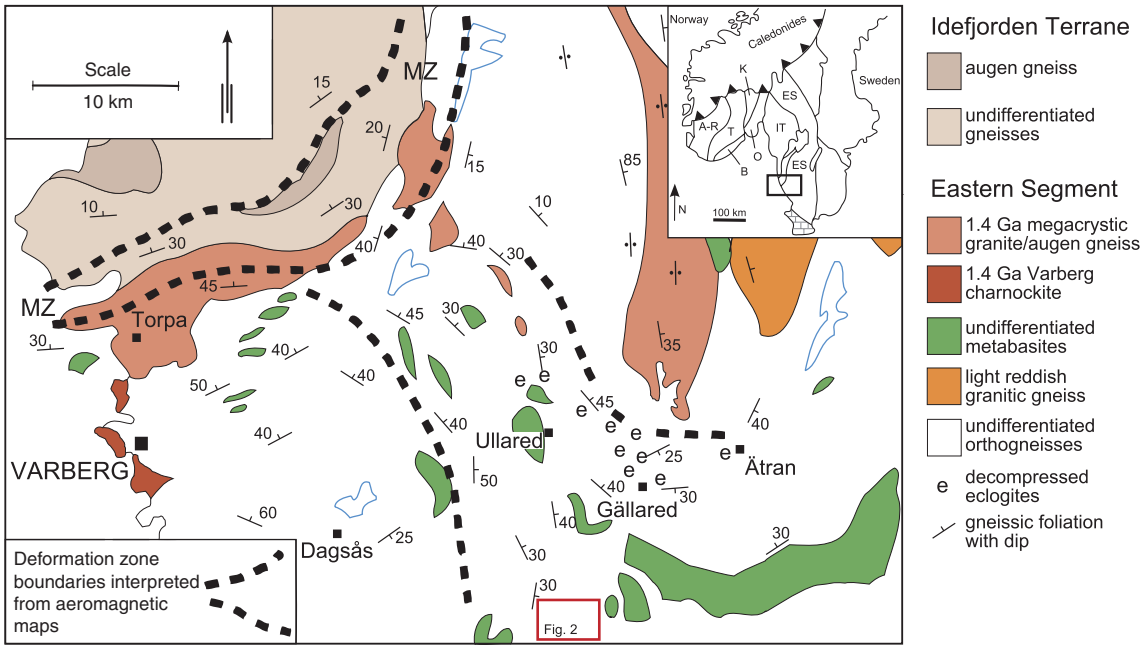

Fig. 1. Geological map of the Varberg–Ullared region (modified after Söderlund et al. 2002). The area mainly consists of undifferentiated orthogneisses with lenses of metabasic rocks and granitic gneisses. It is limited to the north by the Mylonite Zone and is cross cut by minor north-west–south-east-trending deformation zones. Between Ullared, Gällared and Ätran, decompressed eclogites crop out. The frame marks the location of Figure 2. The inset shows the location of the Sveconorwegian orogen in Scandinavia. (A-R = the Rogaland-Agder Terrane, T = the Telemark Terrane, B = the Bamble Terrane, K = the Kongsberg Terrane, O = the Oslo paleo-rift, IT = the Idefjorden Terrane, ES = the Eastern Segment).

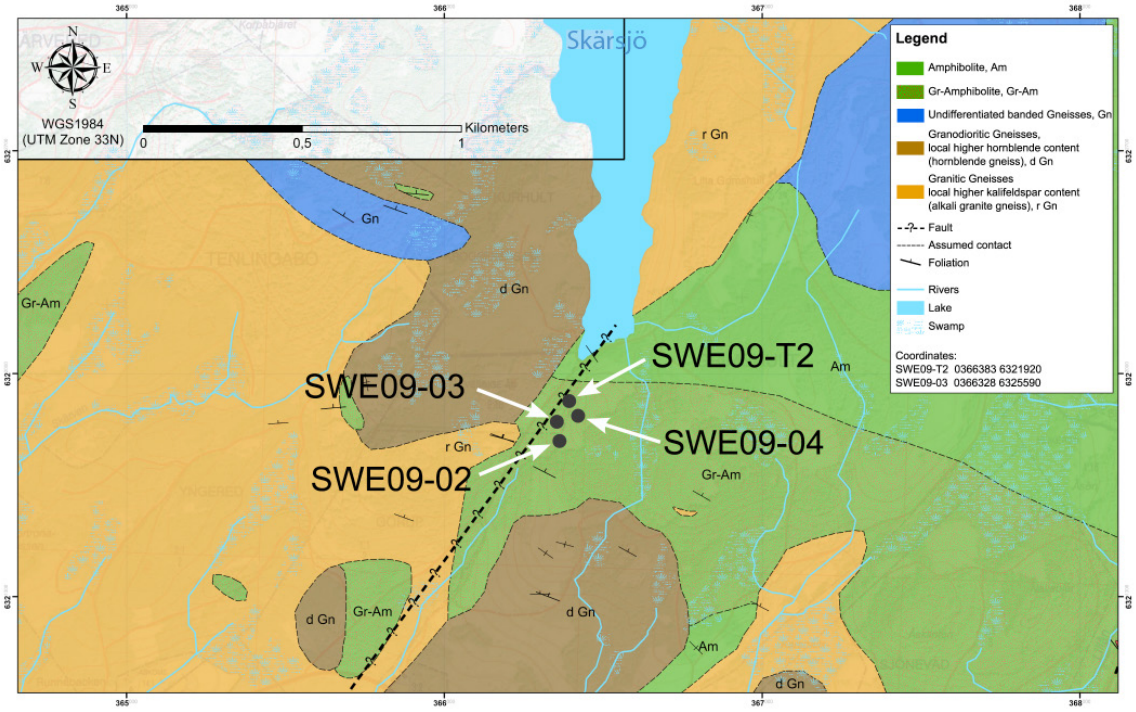

Fig. 2. Detailed map showing the sample localities around lake Skärsjö.

end of the mafic body is cut by a fault. However, there is no clear microscopic and macroscopic evidence of deformation.

The amphibolites vary in grain size, composition and layering. In general, the layered amphibolites consist of equal amounts of medium-grained plagioclase and hornblende together with weathered biotite. The layering consists of alternating hornblende-rich and plagioclase-rich bands.

Garnet is variably distributed and reaches one millimetre in size. Some grains have a white rim of plagioclase and hornblende, suggesting decompression reactions. Furthermore, larger garnets are in some places interconnected via veins composed of plagioclase and quartz, suggesting anatectic formation of a tonalitic melt under high-temperature conditions. Locally, there are more massive amphibolites with coarser, <5 mm hornblende. A few clinopyroxenes show exsolution lamellae of orthopyroxene (sample SWE09-02) and are often altered to hornblende. Minor constituents are biotite, epidote, quartz, olivine, clinopyroxene, orthopyroxene, chlorite, ilmenite and magnetite. Accessory phases are apatite, rutile, zircon and zoisite.

MINERALS AND FABRICS

Two of the samples (SWE09-03 and SWE09-T2) contain relics of magmatic fabrics superposed by high-grade metamorphic mineral growth. Clinopyroxene and epidote are absent in these, and plagioclase-quartz veins are absent at the sample locations.

Large grains of magmatic olivine (on average 0.5–1 mm) and plagioclase (on average 1–2.5 mm) exist next to metamorphic mineral parageneses (Fig. 3A). The magmatic olivines show irregular jointing. Along these small joints, the minerals have been altered by fluids and show fluid-enhanced growth of hornblende and biotite. In some places, a thin rim of newly grown plagioclase surrounds olivine. In addition, small grains of olivine occur together with plagioclase (Figs. 3D, 4B).

The cores of large plagioclase grains were strongly altered to very fine-grained spinel (Fig. 3C), whereas the rims show no signs of alteration. The grains are surrounded by small, euhedral garnets (Fig. 4A). Some of the garnets contain small inclusions of spinel. In addition to the older magmatic plagioclase, newly formed plagioclase is associated with olivine or grew together with garnet. These younger grains show no obvious deformation or alteration.

Moreover, magmatic orthopyroxene can be found. It is altered to hornblende along former exsolution lamellae within the grains and at their edges. In contrast, younger orthopyroxene overgrew olivine and metamorphic garnet. The newly formed hornblende grew under equilibrium conditions (interfacial angles of 60° or 90°, Fig. 3D).

The olivines often occur next to larger orthopyroxenes. In other cases, corona-like structures between olivine and magmatic plagioclase developed (Fig. 3B). Either the olivines have small elongated grains of plagioclase that formed perpendicular to the grain boundaries in turn outwards followed by a rim of small garnets against the magmatic plagioclase relics, or the olivines are surrounded by olivine-garnet symplectites towards the magmatic plagioclase relics.

In addition, ilmenite and magnetite were overgrown by corona-like structures of reddish-brown biotite and brown hornblende often followed by an almost continuous garnet rim.

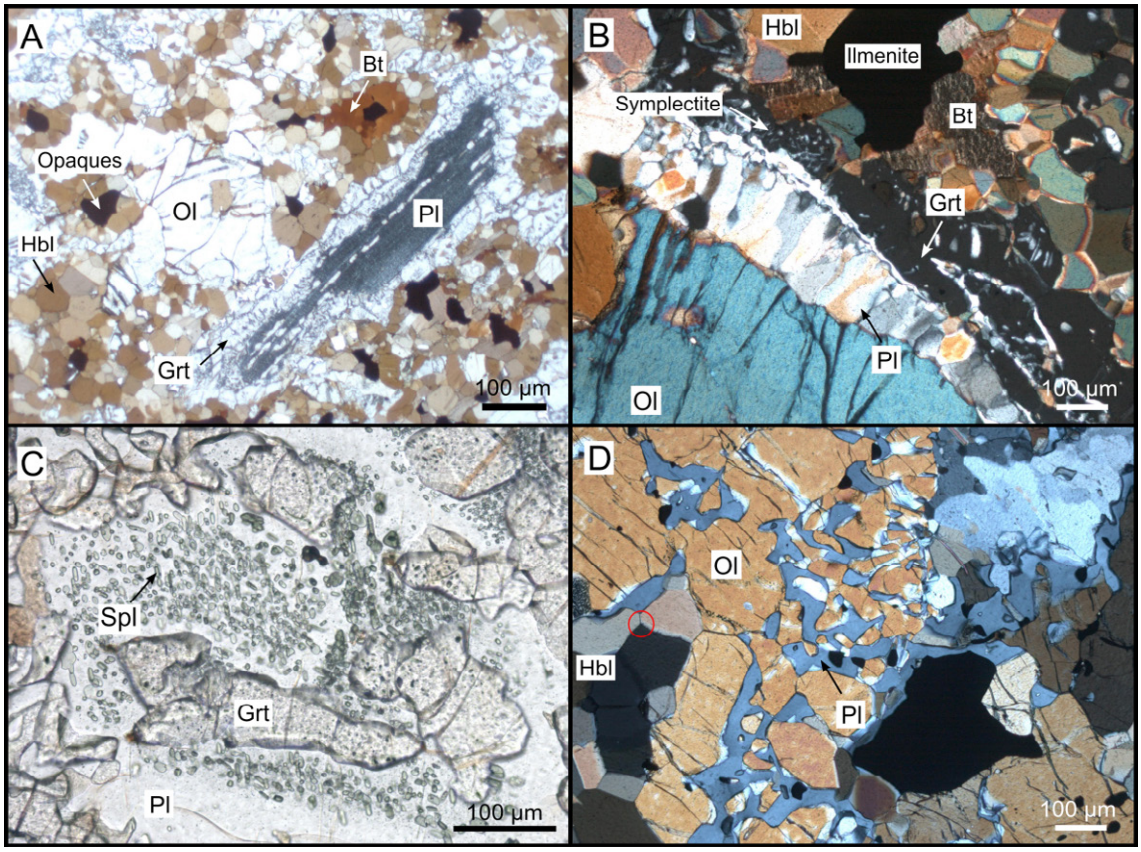

Fig. 3. Thin section photomicrographs of samples SWE09-03 and SWE09-T2. **A.** Magmatic olivine and plagioclase. On the right, a large plagioclase grain is surrounded by small garnets. On the left, there is an olivine with several joints running through the grain. Furthermore, hornblende and biotite are visible, as well as the coronas of biotite and hornblende surrounding opaques. SWE09-03, plane-polarised light. **B.** Reaction rim around olivine. Olivine is surrounded by small elongated grains of plagioclase. They are perpendicular to the grain boundary of olivine and change into plagioclase-garnet symplectites or garnet. In the upper part of the figure, there is another type of corona: An opaque phase is surrounded by biotite and hornblende. SWE09-03, crossed nicols. **C.** Close-up view of spinel in plagioclase. The grains are euhedral and some of them slightly greenish. The inclusion-free plagioclase rim is visible. SWE09-03, plane polarized light. **D.** Close-up view of olivine-plagioclase intergrowth. Plagioclase is located between small olivine relics. In the upper right corner, there is orthopyroxene with minor alterations to hornblende. In the lower left corner, there are several hornblendes with equilibrium fabrics (red circle). SWE09-T2, crossed nicols.

Spinel and pyroxene are not present in this structure. However, larger grains of spinel locally occur together with magnetite.

GEOCHEMISTRY

The bulk rock composition of SWE09-03 was determined by X-ray fluorescence using a PANalytical AXIOS Advanced system (Table 1). The mineral compositions of SWE09-T2 have been determined with a JEOL JXA-8200 electron probe microanalyser (Appendix 1).

The XRF analysis shows that the olivine-bearing amphibolites are conspicuously rich in FeO_{tot} (27 wt.%), TiO_2 (3.6 wt.%) and Ni (244 ppm, Table 1). The SiO_2 concentration is in the range of that of ultrabasic rocks (37.5 wt.%).

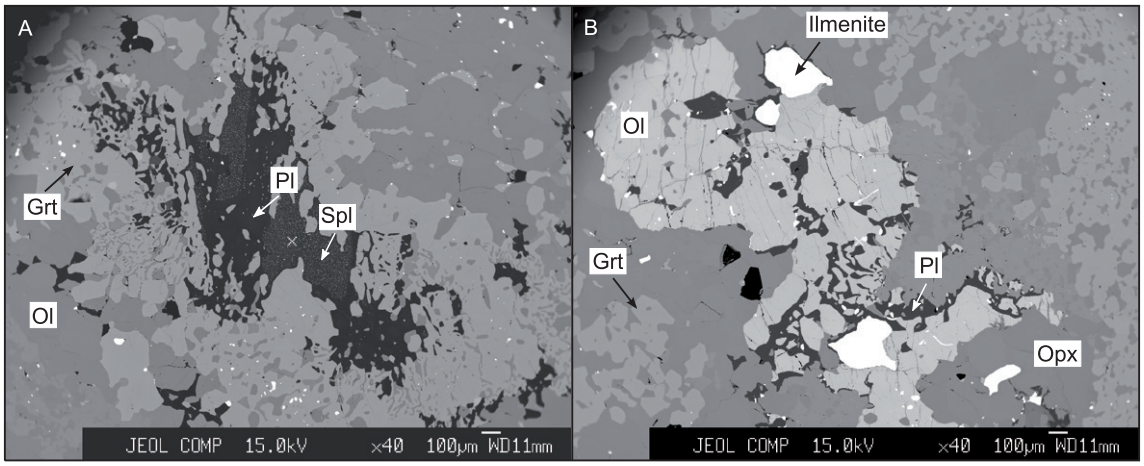

Fig. 4. BSE images of sample SWE09-T2. A. Symplectitic intergrowths of garnet and plagioclase are visible at the left and right side of the magmatic grain. The magmatic plagioclase contains abundant spinel (white dots). B. The olivine grain in the centre is surrounded by a thin plagioclase rim followed by garnet and orthopyroxene. In between there is some ilmenite.

Table 1. Bulk rock chemistry of sample SWE09-03 (XRF analyses).

	Na_2O	Al_2O_3	MnO	FeO	K_2O	SiO_2	MgO	TiO_2	CaO	P_2O_5	Loi	Total
[wt.%]	1.55	11.5	0.238	27.07	0.64	37.5	10.91	3.612	5.35	0.275	1.04	99.72
	Ba	**Cr**	**Ga**	**Nb**	**Ni**	**Rb**	**Sc**	**Sr**	**V**	**Y**	**Zn**	**Zr**
[ppm]	267	428	24	6	244	<3	24	222	702	18	214	121

Olivine occurs as large grains (on average 0.5–1 mm) or as small relics (up to 0.1 mm), both are Fe-rich with 50–55 mole% fayalite. The relics of former magmatic plagioclase have the same composition as the smaller, unaltered grains. All analysed plagioclases have oligoclase compositions ($An_{12–19}$).

The spinel inclusions in plagioclase and garnet, as well as the spinel which coexists with magnetite, are hercynites with variable Cr_2O_3 concentrations. The spinel associated with magnetite contains 1.5 wt.% Cr_2O_3. In contrast, spinel inclusions in plagioclase have Cr_2O_3 concentrations below detection limit (<20 ppm).

The garnets do not show chemical zoning or rim structures. They consist of 56–59 mole% almandine, 28–31 mole% pyrope and 11–12 mole% grossular.

The analysed orthopyroxenes are hypersthene ($En_{61}Fs_{39}$) and there is no difference in composition between magmatic and metamorphic grains. Orthopyroxene compositions clearly vary due to narrow exsolution lamellae. The lamellae are either too thin for analysis or altered to amphibole.

The amphiboles are pargasites and have high TiO_2 contents (3.0–3.6 wt.%). Similarly, biotite has high TiO_2 contents of 5.4–6.3 wt.%.

METAMORPHISM

The garnet-amphibolites contain several indicators of high-grade metamorphic conditions, such as being hypersthene-bearing, suggesting granulite-facies temperatures. The pyrope component of the garnet (28–33%) indicates high pressures. Furthermore, the concentration of titanium in hornblende is typical of high temperature conditions (e.g. Ernst & Liu 1998).

The coronas complicate the identification of the peak mineral parageneses for geothermobarometry. Based on the mineral fabrics, garnet, orthopyroxene, plagioclase and rutile are assumed to have been in equilibrium at peak metamorphic conditions. The calculated temperature is 837–888±75 °C using the garnet-orthopyroxene-thermometer by Aranovich & Berman (1997). The pressure conditions, 8–8.5±0.6 kbar, were calculated using plagioclase-hornblende pairs (Schmidt 1992, Ernst & Liu 1998, Plyusnina 1982). These pressures must be regarded as minimum values since the calculations included hornblende which may not have formed at peak conditions. In addition, the stability field for the garnet-orthopyroxene-plagioclase-rutile±ilmenite paragenesis was calculated by Theriak Domino using the JUN92 database (Fig. 5, grey field). The open-ended P-T field (up to 25 kbar) lies above 670 °C

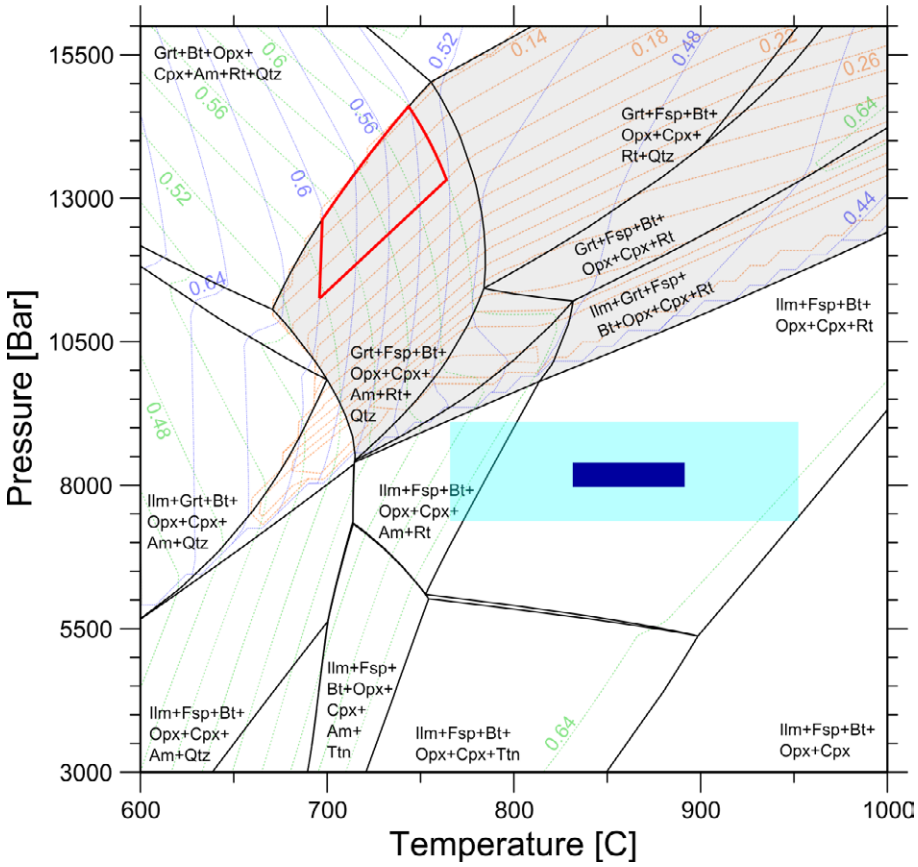

Fig. 5. P-T pseudosection of the mineral parageneses by Theriak Domino using the JUN92 database. The grey field marks the stability field of the grt-opx-pl-rt±ilm paragenesis. The anorthite content of plagioclase (orange lines), almandine content of garnet (blue lines) and magnesium number of orthopyroxene (green lines) restrict the P-T field to 11–14 kbar and 700–750 °C. The results of the grt-opx-thermometer by Aranovich & Berman (1997) are represented by the blue rectangle, and the light blue field marks the range of error for this method. The results of the two methods do not overlap.

and 8 kbar. However, the anorthite content of plagioclase, almandine content of garnet and magnesium number of orthopyroxene restrict the P-T field of the sample to 11–14 kbar and 700–750 °C (Fig. 5, red marks). The P-T conditions, using the garnet-orthopyroxene geothermometer and conventional geobarometers lie below the calculated stability field (Fig. 5, blue rectangle). The conventional geothermobarometers, however, do not take into account high amounts of iron or titanium in the sample and, therefore, the classical approach might not be suitable for these iron-rich rocks. Hence, the lower range of the Theriak Domino data are considered to better represent the conditions, and maximum P-T lies between 11–14 kbar and 700–750 °C.

Biotite (AnnPhl) is retrograde and was formed under lower temperatures and pressure. The various symplectites and well-developed coronas probably indicate slow cooling of the rocks with little deformation. Equilibrium angles between hornblende grains also suggest slow cooling under static conditions.

DISCUSSION

The corona-bearing samples, SWE09-03 and -T2, differ from the other amphibolites samples, SWE09-02 and -04, of our profile (Fig. 3). The latter contain as much opaque minerals but lack olivine and magmatic plagioclase. In the olivine-free amphibolites, clinopyroxene is present and garnets are larger and contain several inclusions. Coronas and alteration of plagioclase to spinel are only observed in the olivine-bearing metagabbros. Clinopyroxene is not present in the coronas and neither are any relics visible, and we assume that it did not take part in the reactions between olivine and plagioclase, although typical olivine coronas are clinopyroxene-bearing (e.g. Griffin & Heier 1973, Whitney & McLelland 1973).

The main difference between the coronas described here and those in the literature is the high FeO_{tot} (27 wt.%) and TiO_2 (3.6 wt.%) contents of the bulk rock. The high fayalite content of olivine (at least 55%) is typical of magmatic olivine, and direct reactions between such olivine and plagioclase to garnet are likely (Green & Hibberson 1970). During such reactions newly formed plagioclase gets lower Ca-concentrations (see equation 1 of Griffin 1973 and equation 2 of Whitney & McLelland 1973). At the same time, the magmatic plagioclase is altered to spinel, releasing Ca (equation 3 of Whitney & McLelland 1973). Both garnet and hornblendes include the released elements. Orthopyroxene may be a reactant and a product in both corona types. Therefore, we suggest the following reactions for the corona formation in the Skärsjö metagabbros:

Fe-olivine + plagioclase → orthopyroxene + garnet (1)

$$4\ MgFeSiO_3 + MgFeAl_2O_4 + CaAl_2Si_2O_8 = (Mg,Fe)_5CaAl_4Si_6O_{24} \quad (2)$$

$$2\ Na^+ + 2\ (Mg,Fe)^{2+} + 3\ CaAl_2Si_2O_8 = 2\ MgFeAl_2O_4 + 3\ Ca^{2+} \quad (3)$$

In contrast to the unchanged composition of the unzoned magmatic olivines, the primary plagioclase should have a higher anorthite content due to the high amount of spinel in the magmatic grains. The formation of spinel requires the availability of high aluminium concentrations (equation 3). Therefore, the spinel is evidence for a primary higher anorthite concentration in the plagioclase cores. Anorthite-rich plagioclase contains more aluminium than albite. The released Ca is taken up by garnet and later hornblende.

Beside plagioclase and orthopyroxene, both magmatic and metamorphic spinels, differing in Cr_2O_3 contents, are present as well. The magmatic spinels contain c. 1.5 wt.% Cr_2O_3 whereas the small metamorphic ones contain nearly no Cr_2O_3.

CONCLUSIONS

The amphibolites of the lake Skärsjö area in the Eastern Segment show olivine-bearing layers next to olivine-free layers. The variations in composition reflect cumulate layers in larger gabbro complexes.

The observed coronas developed only in the olivine-rich layers and are absent in other layers. The coronas surrounding primary magmatic olivine and plagioclase are related to the presence of olivine and high FeO_{tot} concentration of the bulk rock. Olivine is the necessary educt for the reaction between olivine and plagioclase to form metamorphic coronas. In addition, olivine is also part of the reactions forming the hornblende coronas around ilmenite and magnetite. The presence of olivine had also an effect on the alteration of plagioclase to spinel.

The estimated pressures and temperatures (11–14 kbar, 700–750 °C) lie within the range of the high-pressure granulite facies (O'Brien & Rötzler 2003), which is in accordance with the P-T range of the surrounding rocks. Orthopyroxene is still stable under these conditions due to the nearly ultrabasic composition of the host rock. Hence, the localized preservation of magmatic minerals and fabrics are a result of the special compositions of the protolith and not a result of different P-T conditions.

ACKNOWLEDGEMENTS

We would like to thank Charlotte Möller and Jenny Andersson, as well as the Geological Survey of Sweden for giving us the opportunity to conduct our research in southwest Sweden. Furthermore, we would like to thank Christine Fischer for preparing the thin sections and Dr. Christina Günther for her support at the EMPA, as well as Martin Timmerman for English corrections and fruitful suggestions.

REFERENCES

Andersson, J., Möller, C. & Johansson, L., 2002: Zircon geochronology of migmatite gneisses along the Mylonite Zone (S Sweden): a major Sveconorwegian terrane boundary in the Baltic Shield. *Precambrian Research 114*, 121–147.

Andersson, J., Bingen, B., Cornell, D., Johansson, L., Söderlund, U. & Möller, C., 2008: The Sveconorwegian orogen of southern Scandinavia: setting, petrology and geochronology of polymetamorphic high-grade terranes. *33 IGC excursion No 51*, 83 pp.

Aranovich, L.Y. & Berman, R.G., 1997: A new garnet-orthopyroxene thermometer based on reversed Al_2O_3 solubility in FeO-Al_2O_3-SiO_2 orthopyroxene. *American Mineralogist 82*, 345–353.

Bingen, B., Nordgulen, Ø. & Viola, G., 2008a: A four-phase model for the Sveconorwegian orogeny, SW Scandinavia. *Norwegian Journal of Geology 88*, 43–72.

Bingen, B., Anderson, J., Söderlund, U. & Möller, C., 2008b: The Mesoproterozoic in the Nordic countries. *Episodes 31*, 29–34.

Christoffel, C.A., Connelly, J.N. & Åhäll, K.-I., 1999: Timing and characterization of recurrent pre-Sveconorwegian metamorphism and deformation in the Varberg-Halmstad region of SW Sweden. *Precambrian Research 98*, 173–195.

Green, D.H. & Hibberson, W., 1970: The instability of plagioclase in peridotite at high pressure. *Lithos 3*, 209–221.

Griffin, W.L., 1971: Genesis of coronas in anorthosites of the Upper Jotun Nappe, Indre Sogn, Norway. *Journal of Petrology 12*, 219–243.

Griffin, W.L. & Heier, K.S., 1973: Petrological implication of some corona structures. *Lithos 6*, 315–335.

Haas, G.-J.L.M., Nijland, T.G., Valbrecht, P.J., Maijer, C., Verschure, R. & Andersen, T., 2002: Magmatic versus metamorphic origin of olivine-plagioclase coronas. *Contributions to Mineralogy and Petrology 143*, 537–550.

Johnson, C.D. & Carlson, W.D., 1990: The origin of olivine-plagioclase coronas in metagabbros from the Adriondack Mountains, New York. *Journal of Metamorphic Geology 8*, 697–717.

Möller, C., 1998: Decompressed eclogites in the Sveconorwegian (-Grenvillian) orogen of the SW Sweden: petrology and tectonic implications. *Journal of Metamorphic Geology 16*, 641–656.

Möller, C., Anderson, J., Lundqvist, I. & Hellström, F., 2007: Linking deformation, migmatite formation and zircon U-Pb geochronology in polymetamorphic orthogneisses, Sveconorwegian Province, Sweden. Journal of metamorphic Geology 25, 727-750.

O'Brien, P. J. & Rötzler, J., 2003: High-pressure granulites: formation, recovery of peak conditions and implications for tectonics. *Journal of Metamorphic Geology 21*, 3–20.

Söderlund, U., Jarl, L.-G., Persson, P.-O., Stephens, M.B. & Wahlgren, C.-H., 1999: Protolith ages and timing of deformation in the eastern, marginal part of the Sveconorwegian orogen, southwestern Sweden. *Precambrian Research 94*, 29–48.

Söderlund, U., Möller, C., Andersson, J., Johansson, L. & Whitehouse, M., 2002: Zircon geochronology in polymetamorphic gneisses in the Sveconorwegian orogen, SW Sweden: ion microprobe evidence for 1.46–1.42 and 0.98–0.96 Ga reworking. *Precambrian Research 113*, 193–225.

Whitney, P. & McLelland, J.M., 1973: Origin of Coronas in Metagabbros of the Adirondack Mts., NY. *Contributions to Mineralogy and Petrology 39*, 81–98.

Whitney, P.R. & McLelland, J.M., 1983: Origin of biotite-hornblende-garnet coronas between oxides and plagioclase in olivine metagabbros, Adriondack region, New York. *Contributions to Mineralogy and Petrology 82*, 34–41.

APPENDIX 1
Microprobe analysis of olivine, plagioclase, garnet, orthopyroxene, hornblende and biotite of sample SWE09-T2

Mineral	Ol	Ol	Ol	Ol	Ol[a]	Ol[a]	Ol	Ol	Ol	Ol	Ol	Ol
Point	01	02	04	04b	04c	06	08	08b	10	201	202	202b
Na_2O	0.00	0.00	0.01	0.01	0.01	0.00	0.01	0.02	0.02	0.00	0.02	0.00
Al_2O_3	0.01	0.00	0.01	0.00	0.02	0.01	0.01	0.09	0.01	0.00	0.00	0.01
MnO	0.29	0.27	0.25	0.27	0.24	0.22	0.27	0.26	0.18	0.24	0.25	0.28
FeO	42.43	41.94	42.36	42.51	41.62	42.05	43.29	41.90	38.30	45.36	44.68	44.51
K_2O	0.00	0.00	0.00	0.00	0.00	0.00	0.00	0.01	0.02	0.01	0.00	0.00
SiO_2	35.50	35.56	35.37	35.38	35.7	35.20	34.62	18.40	36.82	34.62	35.10	34.85
MgO	22.90	23.50	22.41	22.63	22.72	22.79	21.75	19.25	19.38	22.04	22.45	22.80
TiO_2	0.00	0.00	0.01	0.03	0.03	0.00	0.01	0.03	0.00	0.00	0.00	0.04
Cr_2O_3	0.00	0.04	0.02	0.01	0.02	0.00	0.01	0.01	0.00	0.01	0.00	0.00
CaO	0.00	0.01	0.01	0.01	0.03	0.01	0.02	0.05	0.11	0.01	0.00	0.04
Total	101.13	101.32	100.44	100.83	100.39	100.37	99.98	80.01	94.84	102.28	102.50	102.52
Na	0.00	0.00	0.00	0.00	0.00	0.00	0.00	0.00	0.00	0.00	0.00	0.00
Al	0.00	0.00	0.00	0.00	0.00	0.00	0.00	0.00	0.00	0.00	0.00	0.00
Mn	0.01	0.01	0.01	0.01	0.01	0.01	0.01	0.01	0.00	0.01	0.01	0.01
Fe	1.01	0.99	1.01	1.01	0.99	1.01	1.05	0.95	0.95	1.08	1.06	10.5
K	0.00	0.00	0.00	0.00	0.00	0.00	0.00	0.00	0.00	0.00	0.00	0.00
Si	1.01	1.01	1.01	1.01	1.02	1.01	1.00	0.73	1.09	0.99	0.99	0.99
Mg	0.97	0.99	0.96	0.96	0.96	0.97	0.94	1.14	0.86	0.94	0.95	0.96
Ti	0.00	0.00	0.00	0.00	0.00	0.00	0.00	0.00	0.00	0.00	0.00	0.00
Cr	0.00	0.00	0.00	0.00	0.00	0.00	0.00	0.00	0.00	0.00	0.00	0.00
Ca	0.00	0.00	0.00	0.00	0.00	0.00	0.00	0.00	0.00	0.00	0.00	0.00
Fa	0.51	0.50	0.51	0.51	0.51	0.53	0.55	0.53	0.51	0.54	0.53	0.54

Mineral	Ol	Ol	Ol	Ol	Ol	Ol	Ol	Ol	Ol	Ol	Ol
Point	204	205	205b	206	206b	207	208	208b	209	210	210b
Na_2O	0.00	0.01	0.00	0.00	0.02	0.00	0.00	0.01	0.00	0.00	0.00
Al_2O_3	0.00	0.04	0.00	0.00	0.01	0.00	0.00	0.00	0.00	0.00	0.00
MnO	0.22	0.22	0.23	0.26	0.26	0.27	0.21	0.20	0.29	0.23	0.24
FeO	45.79	45.88	45.49	44.52	45.27	45.15	45.23	45.77	45.69	46.00	45.73
K_2O	0.01	0.00	0.00	0.00	0.00	0.00	0.00	0.00	0.00	0.00	0.00
SiO_2	34.76	34.94	34.80	34.81	34.85	35.03	34.84	34.67	34.81	34.66	34.46
MgO	21.89	22.06	22.02	22.89	22.78	22.88	22.44	22.14	22.11	22.08	21.75
TiO_2	0.00	0.00	0.01	0.00	0.01	0.02	0.00	0.01	0.01	0.01	0.00
Cr_2O_3	0.00	0.05	0.02	0.00	0.00	0.00	0.00	0.01	0.02	0.01	0.00
CaO	0.02	0.01	0.02	0.00	0.01	0.00	0.01	0.01	0.01	0.02	0.01
Total	102.70	103.20	102.58	102.49	103.202	103.34	102.73	102.82	102.94	103.00	102.19
Na	0.00	0.00	0.00	0.00	0.00	0.00	0.00	0.00	0.00	0.00	0.00
Al	0.00	0.00	0.00	0.00	0.00	0.00	0.00	0.00	0.00	0.00	0.00
Mn	0.01	0.01	0.01	0.01	0.01	0.01	0.00	0.00	0.01	0.01	0.01
Fe	1.09	1.08	1.08	1.05	1.07	1.06	1.07	1.09	1.08	1.09	1.09
K	0.00	0.00	0.00	0.00	0.00	0.01	0.02	0.03	0.04	0.05	0.06
Si	0.99	0.99	0.99	0.99	0.99	0.99	0.99	0.99	0.99	0.99	0.99
Mg	0.93	0.93	0.93	0.97	0.96	0.96	0.95	0.94	0.93	0.93	0.93
Ti	0.00	0.00	0.00	0.00	0.00	0.00	0.00	0.00	0.00	0.00	0.00
Cr	0.00	0.00	0.00	0.00	0.00	0.00	0.00	0.00	0.00	0.00	0.00
Ca	0.00	0.00	0.00	0.00	0.00	0.00	0.00	0.00	0.00	0.00	0.00
Fa	0.54	0.54	0.52	0.53	0.53	0.53	0.54	0.54	0.54	0.54	0.52

a Symplectitic intergrowth

Mineral	Pl	Pl[a]	Pl	Pl[a]	Pl[c]	Pl	Pl	Pl[b]	Pl	Pl[c]
Point	04	06	08	10	11	11b	202	203	203b	204
Na_2O	10.24	10.18	10.08	10.35	10.20	10.30	9.18	9.68	9.81	8.96
Al_2O_3	22.103	21.16	22.24	22.03	21.72	21.82	23.21	22.37	22.12	23.14
MnO	0.00	0.00	0.00	0.02	0.00	0.00	0.00	0.00	0.00	0.02
FeO	0.32	1.15	0.20	0.21	0.08	0.31	0.16	0.21	0.66	0.07
K_2O	0.07	0.10	0.19	0.12	0.17	0.18	0.04	0.08	0.08	0.20
SiO_2	65.00	65.04	64.12	65.39	64.51	65.00	63.96	64.53	65.23	63.08
MgO	0.01	0.25	0.00	0.00	0.00	0.01	0.05	0.00	0.01	0.00
TiO_2	0.03	0.00	0.01	0.00	0.03	0.01	0.01	0.00	0.00	0.00
Cr_2O_3	0.01	0.00	0.01	0.00	0.02	0.00	0.02	0.00	0.01	0.00
CaO	2.98	2.50	2.65	2.65	2.61	2.65	3.69	2.95	2.64	3.80
Total	100.75	100.36	99.83	100.77	99.33	100.28	100.23	99.82	100.58	99.26
Na	0.87	0.87	0.86	0.88	0.88	0.88	0.78	0.83	0.83	0.77
Al	1..14	1.09	1.15	1.14	1.12	1.13	1.20	1.16	1.14	1.19
Mn	0.00	0.00	0.00	0.00	0.00	0.00	0.00	0.00	0.00	0.00
Fe	0.01	0.04	0.01	0.01	0.00	0.01	0.01	0.01	0.02	0.00
K	0.00	0.01	0.01	0.01	0.01	0.01	0.00	0.00	0.00	0.01
Si	2.85	2.85	2.81	2.87	2.83	2.85	2.80	2.83	2.86	2.76
Mg	0.00	0.02	0	0.00	0.00	0.00	0.00	0.00	0.00	0.00
Ti	0.00	0.00	0.00	0.00	0.00	0.00	0.00	0.00	0.00	0.00
Cr	0.00	0.00	0.00	0.00	0.00	0.00	0.00	0.00	0.00	0.00
Ca	0.14	0.12	0.14	0.12	0.12	0.12	0.17	0.14	0.12	0.18
Ab	0.86	0.88	0.85	0.87	0.87	0.87	0.82	0.85	0.87	0.80
An	0.14	0.12	0.14	0.12	0.12	0.12	0.18	0.14	0.13	0.19

Mineral	Pl	Pl	Pl	Pl	Pl[b]	Pl[b]	Pl[b]	Pl[b]	Pl	Pl[a]
Point	204b	204c	205	205b	206	206b	208	208b	209	210
Na_2O	9.74	9.30	9.74	9.54	9.63	9.76	9.58	9.77	9.55	9.48
Al_2O_3	22.31	22.96	22.43	22.59	22.16	22.28	22.24	22.04	22.13	22.62
MnO	0.00	0.00	0.00	0.01	0.00	0.01	0.00	0.00	0.00	0.00
FeO	0.29	0.43	0.30	0.17	0.42	0.48	0.35	0.33	0.29	0.61
K_2O	0.26	0.17	0.17	0.17	0.11	0.11	0.19	0.17	0.07	0.12
SiO_2	65.13	63.55	64.92	64.74	65.02	64.48	64.78	65.00	65.22	64.08
MgO	0.01	0.03	0.00	0.00	0.00	0.00	0.09	0.01	0.02	0.01
TiO_2	0.00	0.03	0.03	0.00	0.00	0.00	0.02	0.01	0.02	0.00
Cr_2O_3	0.01	0.00	0.01	0.00	0.01	0.00	0.00	0.00	0.00	0.00
CaO	2.54	3.40	2.69	2.86	2.67	2.75	2.63	2.46	2.65	3.20
Total	100.29	99.86	100.29	100.08	100.02	99.89	99.86	99.78	99.95	100.13
Na	0.83	0.80	0.83	0.81	0.82	0.84	0.82	0.84	0.81	0.81
Al	1.15	1.19	1.16	1.17	1.14	1.15	1.15	1.14	1.14	1.17
Mn	0.00	0.00	0.00	0.00	0.00	0.00	0.00	0.00	0.00	0.00
Fe	0.01	0.02	0.01	0.01	0.02	0.02	0.01	0.01	0.01	0.02
K	0.01	0.01	0.01	0.01	0.01	0.01	0.01	0.01	0.00	0.01
Si	2.85	2.78	2.84	2.84	2.85	2.83	2.84	2.85	2.86	2.81
Mg	0.00	0.00	0.00	0.00	0.00	0.00	0.00	0.00	0.00	0.00
Ti	0.00	0.00	0.00	0.00	0.00	0.00	0.00	0.00	0.00	0.00
Cr	0.00	0.00	0.00	0.00	0.00	0.00	0.00	0.00	0.00	0.00
Ca	0.12	0.16	0.13	0.13	0.13	0.13	0.12	0.12	0.12	0.15
Ab	0.86	0.83	0.86	0.85	0.86	0.86	0.86	0.87	0.86	0.84
An	0.12	0.17	0.13	0.14	0.13	0.13	0.13	0.12	0.13	0.16

a Symplectitic intergrowth

b Rim

c Magmatic grain

Mineral	Grt	Grt	Grt	Grt[a]	Grt[a]	Grt	Grt	Grt	Grt	Grt	Grt
Point	02	05	05b	09	10	11	11b	204	204b	204c	209
Na_2O	0.00	0.02	0.00	0.02	0.03	0.02	0.03	0.03	0.02	0.02	0.00
Al_2O_3	22.61	22.45	22.67	22.30	22.51	22.60	22.42	23.29	23.30	23.43	23.14
MnO	0.74	0.74	0.75	0.77	0.79	0.72	0.71	0.70	0.68	0.65	0.77
FeO	26.63	26.56	26.42	27.16	26.57	26.34	26.30	28.00	28.26	28.07	28.65
K_2O	0.00	0.00	0.00	0.00	0.00	0.00	0.00	0.00	0.01	0.00	0.00
SiO_2	39.24	39.29	39.80	39.31	39.16	39.45	39.85	39.44	39.19	39.50	39.17
MgO	7.99	7.88	8.04	7.24	7.62	7.89	7.91	8.19	7.99	8.07	7.81
TiO_2	0.04	0.02	0.05	0.01	0.05	0.01	0.03	0.01	0.04	0.05	0.05
Cr_2O_3	0.02	0.02	0.01	0.02	0.00	0.02	0.01	0.00	0.00	0.01	0.02
CaO	4.07	4.01	4.20	4.25	3.90	4.29	4.19	4.08	3.98	4.08	3.98
Total	101.34	101.00	101.95	101.13	100.62	101.34	101.45	103.74	103.46	103.89	103.59
Na	0.00	0.00	0.00	0.00	0.00	0.00	0.00	0.00	0.00	0.00	0.00
Al	2.03	2.01	2.03	2.00	2.02	2.03	2.01	2.09	2.09	2.10	2.08
Mn	0.05	0.05	0.05	0.05	0.05	0.05	0.05	0.05	0.04	0.04	0.05
Fe	1.69	1.69	1.68	1.73	1.69	1.68	1.67	1.78	1.80	1.79	1.82
K	0.00	0.00	0.00	0.00	0.00	0.00	0.00	0.00	0.00	0.00	0.00
Si	2.99	2.99	3.03	2.99	2.98	3.00	3.03	3.00	2.98	3.01	2.98
Mg	0.91	0.89	0.91	0.82	0.86	0.90	0.90	0.93	0.91	0.92	0.89
Ti	0.00	0.00	0.00	0.00	0.00	0.00	0.00	0.00	0.00	0.00	0.00
Cr	0.00	0.00	0.00	0.00	0.00	0.00	0.00	0.00	0.00	0.00	0.00
Ca	0.33	0.33	0.34	0.35	0.32	0.35	0.34	0.33	.32	0.33	0.32
Fe^{2+}	1.69	1.69	1.68	1.73	1.69	1.68	1.67	1.78	1.80	1.79	1.82
Fe^{3+}	0.00	0.00	0.00	0.00	0.00	0.00	0.00	0.00	0.00	0.00	0.00
Alm	0.57	0.57	0.56	0.59	0.58	0.56	0.57	0.58	0.59	0.58	0.59
Prp	0.30	0.30	0.31	0.28	0.30	0.30	0.30	0.30	0.30	0.30	0.29
Grs	0.11	0.11	0.11	0.12	0.11	0.12	0.12	0.11	0.11	0.11	0.11

Mineral	Opx[a]	Opx[a]	Opx[c]	Opx
Point	09	205	208	208b
Na_2O	0.00	0.03	0.01	0.01
Al_2O_3	1.66	1.49	1.47	1.54
MnO	0.23	0.17	0.22	0.23
FeO	22.28	25.25	25.48	25.58
K_2O	0.01	0.00	0.00	0.01
SiO_2	52.90	52.87	52.54	52.15
MgO	22.90	21.51	21.57	21.37
TiO_2	0.09	0.09	0.08	0.05
Cr_2O_3	0.00	0.04	0.00	0.01
CaO	0.24	0.28	0.19	0.21
Total	100.31	101.73	101.56	101.15
Na	0.00	0.00	0.00	0.00
Al	0.07	0.06	0.06	0.07
Mn	0.01	0.01	0.01	0.01
Fe	0.69	0.78	0.79	0.80
K	0.00	0.00	0.00	0.00
Si	1.06	1.96	195	1.95
Mg	1.26	1.19	1.19	1.19
Ti	0.00	0.00	0.00	0.00
Cr	0.00	0.00	0.00	0.00
Ca	0.01	0.01	0.01	0.01
En	0.65	0.60	0.60	0.60
Fs	0.35	0.40	0.40	0.40

a Symplectitic intergrowth

c Magmatic grain

Mineral	Hbl	Hbl	Hbl	Hbl	Hbl	Hbl	Hbl	Hbl	Hbl	Hbl	Hbl
Point	04	05	08	10	11	202	202b	204	204b	206	210
Na_2O	3.61	3.51	3.63	3.77	3.77	3.48	3.36	3.50	3.59	3.53	3.57
Al_2O_3	13.98	13.74	13.50	13.55	13.60	13.45	13.21	13.62	13.97	14.04	13.86
MnO	0.07	0.04	0.10	0.06	0.06	0.12	0.12	0.06	0.12	0.04	0.09
FeO	12.61	13.36	15.50	15.28	14.53	15.46	15.05	16.49	15.93	15.84	16.38
K_2O	0.78	0.83	0.77	0.75	0.72	0.78	0.80	0.75	0.77	0.75	0.73
SiO_2	40.90	41.75	41.41	40.17	41.24	41.11	41.24	40.27	41.00	40.85	41.30
MgO	10.23	11.33	10.30	10.38	10.89	10.39	10.74	9.84	10.67	10.16	10.21
TiO_2	3.60	3.64	3.40	3.06	3.14	3.77	3.46	3.28	3.12	3.50	3.41
Cr_2O_3	0.10	0.02	0.05	0.03	0.02	0.12	0.14	0.08	0.02	0.06	0.09
CaO	9.86	10.16	9.46	9.58	9.69	10.01	9.56	9.74	9.64	10.10	9.58
Total	97.72	98.38	98.12	96.52	97.64	98.68	97.98	97.64	98.84	98.87	99.22
Na	1.04	1.00	1.05	1.11	1.09	1.00	0.97	1.02	1.03	1.01	1.02
Al	2.46	2.38	2.37	2.40	2.39	2.35	2.32	2.42	2.44	2.45	2.41
Mn	0.01	0.01	0.01	0.01	0.01	0.01	0.02	0.01	0.02	0.01	0.01
Fe	1.82	1.65	1.93	1.94	1.81	1.92	1.88	2.08	1.98	1.97	2.03
K	0.15	0.16	0.15	0.15	0.14	0.15	0.15	0.14	0.15	0.14	0.14
Si	6.10	6.15	6.17	6.10	6.15	6.10	6.15	6.07	6.08	6.06	6.11
Mg	2.27	2.49	2.29	2.35	2.42	2.30	2.39	2.12	2.36	2.25	2.25
Ti	0.40	0.40	0.38	0.35	0.35	0.42	0.39	0.37	0.35	0.39	0.38
Cr	0.02	0.00	0.01	0.01	0.00	0.02	0.02	0.01	0.00	0.01	0.02
Ca	1.58	1.60	1.51	1.56	1.55	1.59	1.57	1.57	1.53	1.61	1.52

Mineral	Bt	Bt	Bt
Point	204	204b	206
Na_2O	0.74	0.75	0.72
Al_2O_3	15.17	15.02	15.47
MnO	0.00	0.02	0.03
FeO	16.54	17.12	16.47
K_2O	9.01	9.02	8.44
SiO_2	36.28	36.42	36.20
MgO	12.94	12.71	13.85
TiO_2	5.82	6.25	5.50
Cr_2O_3	0.12	0.11	0.08
CaO	0.00	0.00	0.00
Total	96.61	97.41	96.75
Na	0.12	0.012	0.11
Al	1.36	1.35	1.39
Mn	0.00	0.01	0.02
Fe	1.05	1.09	1.05
K	0.88	0.88	0.82
Si	2.76	2.77	2.75
Mg	1.47	1.44	1.57
Ti	0.33	0.36	0.32
Cr	0.01	0.01	0.01
Ca	0.00	0.00	0.00